Quercetin ameliorates dysregulation of lipid metabolism genes via the PI3K/AKT pathway in a diet-induced mouse model of non-alcoholic fatty liver disease

Sandra Pisonero-Vaquero[1], Ángel Martínez-Ferreras[1], María Victoria García-Mediavilla[1,2], Susana Martínez-Flórez[1], Anna Fernández[1], Marta Benet[2,3], José Luis Olcoz[2,4], Ramiro Jover[2,3,5], Javier González-Gallego[1,2] and Sonia Sánchez-Campos[1,2]

[1]Institute of Biomedicine (IBIOMED), University of León, León, Spain; [2]Centro de Investigación Biomédica en Red de Enfermedades Hepáticas y Digestivas (CIBERehd), Instituto de Salud Carlos III, Madrid, Spain; [3]Experimental Hepatology Unit, IIS Hospital La Fe, Valencia, Spain; [4]Department of Gastroenterology. Complejo Asistencial Universitario de León, León, Spain; [5]Department of Biochemistry and Molecular Biology, University of Valencia, Valencia, Spain.

Correspondence: Sonia Sánchez-Campos, Institute of Biomedicine, University of León, Campus de Vegazana, 24071 León, Spain.

E-mail: ssanc@unileon.es

Fax: +34987291267

Abbreviations: ALT, alanine aminotransferase; AST, aspartate aminotransferase; C/EBPα, CCAAT/enhancer binding protein alpha; C/EBPβ, CCAAT/enhancer binding protein beta; FABP1, fatty acid binding protein 1; FAT/CD36, fatty acid translocase CD36; FATP5, fatty acid transport protein 5; FFA, free fatty acid; FOXA1, forkhead box protein A1; GAPDH, glyceraldehyde-3-phosphate dehydrogenase; iNOS, inducible nitric oxide synthase; LXRα, liver X receptor alpha; MCD, methionine and choline

deficient; NAFLD, non-alcoholic fatty liver disease; NAS, NAFLD activity score; NASH, non-alcoholic steatohepatitis; OPN, osteopontin; PI3K, phosphatidylinositol 3-kinase; PPARα, peroxisome proliferator-activated receptor alpha; RNS, reactive nitrogen species; ROS, reactive oxygen species; SHP; small heterodimer partner; SOCS3, suppressor of cytokine signaling 3; SREBP-1c, sterol regulatory element binding protein 1c; TC, total cholesterol; TG, triglycerides; TNFα; tumor necrosis factor.

Keywords: Fatty acid uptake, lipid metabolism, NAFLD, PI3K/AKT pathway, quercetin.

Abstract

Scope: Flavonoids and related compounds seem to have favorable effects on non-alcoholic fatty liver disease (NAFLD) progression, although the exact mechanisms implicated are poorly understood. In this study, we aimed to investigate the effect of the flanovol quercetin on gene expression deregulation involved in the development of NAFLD, as well as the possible implication of phosphatidylinositol 3-kinase (PI3K)/AKT pathway modulation.

Methods and results: We used an *in vivo* model based on methionine and choline deficient (MCD) diet-fed mice and an *in vitro* model consisting of Huh7 cells incubated with MCD medium. MCD-fed mice showed classical pathophysiological characteristics of non-alcoholic steatohepatitis (NASH), associated with altered transcriptional regulation of fatty acid uptake- and trafficking-related gene expression, with increased lipoperoxidation. PI3K/AKT pathway was activated by MCD and triggered gene deregulation causing either activation or inhibition of all studied genes as demonstrated through cell incubation with the PI3K inhibitor LY294002. Treatment with quercetin reduced AKT phosphorylation and oxidative/nitrosative stress, inflammation and lipid metabolism-related genes displayed a tendency to normalize in both *in vivo* and *in vitro* models.

Conclusion: These results place quercetin as a potential therapeutic strategy for preventing NAFLD progression by attenuating gene expression deregulation, at least in part through PI3K/AKT pathway inactivation.

1. Introduction

Non-alcoholic fatty liver disease (NAFLD) is one of the most common chronic liver diseases in the Western countries, considered the hepatic manifestation of the metabolic syndrome [1]. It ranges from simple steatosis to steatohepatitis, liver fibrosis, cirrhosis and hepatocellular carcinoma [2]. NAFLD is characterized by the accumulation of triglycerides in the liver, caused by multiple factors, as the increment of fatty acid uptake as a result of the enhancement of the lipolysis from the adipocytes or the increased intake of dietary fat. Additionally, increased *de novo* lipogenesis, decreased fatty acid oxidation and reduced very low density lipoprotein secretion contribute to this phenomenon [3]. However, the accumulation of triglycerides in droplets may be protective and free fatty acids in the liver can serve as substrates for formation of nontriglyceride lipotoxic metabolites that cause actually the liver injury [4].

The fatty acid translocase (FAT)/CD36 is a membrane protein implicated in fatty acid uptake and its upregulation is associated with insulin resistance, hyperinsulinemia and fat accumulation in NAFLD [5]. A key regulator of fatty acid trafficking and partition in the liver that protects the cells against lipotoxicity is the fatty acid binding protein (FABP)1. In this regard, we have recently described the important role of FABP1 downregulation in the pathogenesis of NAFLD in *in vivo* models as well as in patients [6], contributing to free fatty acid lipotoxicity and lipid accumulation in this disease.

Most therapeutic approaches for NAFLD target the major pathways thought to be essential in the pathogenesis of nonalcoholic steatohepatitis and are often directed at reducing body mass index and improving insulin resistance via pharmacologic, surgical, dietary, or exercise regimens [7]. Nevertheless, there is an increasing scientific interest in new treatments based on the modulation of key pathways implicated in lipid metabolism, including the use of natural compounds. Thus, polyphenols such as

curcumin and silibinin are able to improve liver histology in different models of NAFLD by modulating the expression of genes related with lipid homeostasis, oxidative stress and inflammation [8,9].

Flavonoids are a large class of naturally occurring compounds widely present in fruits, vegetables and beverages derived from plants. There is an increasing evidence that intake of flavonoids and related compounds can have favorable effects on cancers and chronic diseases, including cardiovascular disease, type II diabetes and NAFLD, at least in part through the immunomodulatory, anti-inflammatory and antioxidant properties of these compounds [10-12]. Quercetin is one of the most abundant flavonoids that presents a wide variety of biological functions. Beneficial effects of this flavonol have been reported on lipid accumulation, inflammation, fibrosis, nitrosative/oxidative stress and insulin resistance associated to NAFLD [11,13,14]. Nevertheless, the exact mechanisms implicated in these multiple actions of quercetin are poorly understood.

In the present study, we aimed to investigate the mechanisms underlying the relationship between the oxidative/nitrosative, inflammatory and lipid metabolism-related gene deregulation associated with NAFLD and the effect of a treatment with quercetin in this complex genomic framework using *in vivo* and *in vitro* models of NAFLD.

2. Materials and methods

2.1. Animals and treatments

Male C57BL/6J mice (8–10 weeks old) were fed with a standard diet and once they had adapted to the environment were distributed in 4 groups: MCD group was fed a methionine- and choline- deficient (MCD) diet to induce NAFLD; Control group received the same MCD diet supplemented with DL-methionine (3 g/kg) and choline

chloride (2 g/kg); MCD Q group was fed with MCD diet supplemented with aglycone quercetin (0.05% w/w); Control Q group was fed with MCD diet supplemented with DL-methionine (3 g/kg), choline chloride (2 g/kg) and aglycone quercetin (0.05% w/w, ssniff Spezialdiäten GmbH, Soest, Germany). Mice were housed in a room under controlled temperature, humidity and lighting and allowed food and water ad libitum up to 4 weeks (W). Body weight and food intake were measured every week. At the end of second, third and fourth week, mice (six of each group) were euthanized, plasma collected and liver excised and weighed. A part of the right posterior lobe was fixed in 10% formalin and the remaining liver was snap frozen.

All animal studies were approved by the local Animal Ethics Committees in accordance with the guidelines of European Research Council for animal care and use.

2.2. Histopathology and immunofluorescence

Liver tissue samples fixed in 10% formalin were embedded in paraffin, sectioned and stained with hematoxylin and eosin (H&E). Lesions were evaluated by a histological scoring system for non-alcoholic fatty liver disease proposed by Kleiner *et al.* [15]. The NAFLD activity score (NAS) comprised 3 histological features which were evaluated semi-quantitatively: steatosis (0-3), lobular inflammation (0-3) and hepatocellular ballooning (0-2). Samples of >5 correlated with a diagnosis of steatohepatitis (NASH), and samples with scores of less than 3 were diagnosed as “not NASH.” Histological analysis of all samples was performed by two independent expert examiners blinded to experimental design data. Snap frozen liver tissue samples were sectioned and stained with either 3% Oil Red O (Sigma-Aldrich, Madrid, Spain) or 1 μg/ml Bodipy 493/503 and Bodipy 581/591 C_{11} (Invitrogen, Carlsbad, CA, USA) combined with DAPI for

nuclei staining, to analyze lipid accumulation or lipid accumulation and lipoperoxidation, respectively.

Snap frozen liver tissue sections were also incubated with rabbit anti-FAT/CD36 antibody (Santa Cruz Biotechnology, Santa Cruz, CA, USA) at 4°C overnight. Thereafter, the secondary antibody donkey anti-rabbit conjugated to Cy3 (Jackson ImmunoResearch, Baltimore, PA, USA) was applied and next lipid droplets and nuclei were stained with 1 μg/ml Bodipy 493/503 and DAPI, respectively.

All sections were examined using a Nikon Eclipse Ti inverted microscope (Nikon, Amstelveen, The Netherlands).

2.3. Biochemical analysis

Plasma levels of total cholesterol (TC), LDL, HDL, triglycerides (TG), alanine aminotransferase (ALT), aspartate aminotransferase (AST), glucose and albumin were determined by the Instrumental Techniques Laboratory of the University of León using standard techniques.

2.4. Triglyceride and free fatty acid assay

Liver triglyceride (TG) and free fatty acid (FFA) contents were determinate after tissue homogenization by using kits from Biovision Research Products (Mountain View, CA, USA) following the guide provided by the company.

2.5. Cells, cell culture and treatment protocols

Huh7 cells were grown at 37 ºC with a 5% CO_2 atmosphere in DMEM/F12 medium (Life Technologies, Carlsbad, CA, USA), supplemented with 10% fetal calf serum and

50 mg/ml gentamycin. In order to prevent phenotypic drift, the cultures were used for only 8–10 weeks before reverting to frozen stocks from an early passage.

MCD medium has previously been reported to induce lipid accumulation in human and murine hepatocytes [16,17]. After serum starvation for 24 hours Huh7 cells were incubated with either control medium (Control) or identical medium deficient of methionine and choline (MCD medium), supplemented or not with aglycone quercetin (Control Q and MCD Q, respectively) (Sigma-Aldrich) at 10 μM for 24 hours to evaluate its effect on oxidative/nitrosative stress, inflammation, lipoperoxidation and lipid accumulation. We also investigated the effect of phosphatidylinositol 3-kinase (PI3K) chemical inhibition by incubating MCD- and MCD Q-treated Huh7 cells with 50 μM LY294002 (Tocris Bioscience, Bristol, UK) during the last 8h of treatment. The vehicle used for all treatments was DMSO; non-treated cells were incubated at the same DMSO concentration (0.05%).

2.6. Cell viability in cell culture

The cell viability was assessed by the mitochondrial function, measured by 3-(4,5-dimethylthiazol-2-yl)-2,5-diphenyltetrazolium bromide (MTT) reduction activity for measuring cell proliferation and cytotoxicity as previously reported [18]. Briefly, cells were seeded in a 24-well plate and incubated with the different treatments. After that, the cells were treated with 0.5 mg/mL MTT (Sigma-Aldrich) for 2 h at 37 ºC. Subsequently, the media were aspirated and the cells were lysed with DMSO, where after the absorbance was read at 560 nm, with background subtraction at 650 nm, using a microplate reader (Bio-Rad Laboratories, Veenendaal, The Netherlands).

2.7. Flow cytometry and fluorescence microscopy

Reactive oxygen and nitrogen species (ROS/RNS) production and lipid peroxidation in cultured cells were analyzed by flow cytometry. The ROS and RNS production was assessed as the fluorescence of 2',7'-dichlorofluorescein (DCF), which is the oxidation product of 2',7'-dichlorodihydrofluorescein diacetate (DCFH-DA; Sigma-Aldrich) with a sensitivity for H_2O_2/NO-based radicals [19]. The lipid peroxidation was determined using Bodipy 581/591 C_{11} (Invitrogen). Briefly, cell monolayers were washed twice with PBS and incubated with the corresponding dye solution (5 μM for DCFH-DA or 1 μg/ml for Bodipy 581/591 C_{11}) for 30 minutes at 37°C, then washed twice, resuspended in PBS, and analyzed on a FACSCalibur flow cytometer (Becton Dickinson Biosciences, San Jose, CA, USA). Fluorescence of 10,000 cells was assessed using Cell Quest software (Becton Dickinson Biosciences). Lipid peroxidation was also examined by fluorescence microscopy, as well as lipid accumulation and fatty acid uptake, using Bodipy 581/591 $C_{11,}$ Bodipy 493/503 and Bodipy FL C_{12} (Invitrogen), respectively. Cell monolayers were fixed in 3.7% paraformaldehyde for 20 minutes at room temperature and incubated with 1 μg/ml Bodipy 581/591 C_{11} or Bodipy 493/503 for 30 minutes at room temperature. For fatty acid uptake assay, Bodipy FL C_{12} was added to cell culture at the beginning of the treatments and cells were fixed at 0, 8 and 24 hours after dye addition. Nuclei were stained with DAPI. All fluorescence images were acquired using a Nikon Eclipse Ti inverted microscope (Nikon) [12].

2.8. Quantitative Real-Time PCR

Total RNA was obtained by using a Trizol reagent (Life Technologies). First-strand cDNA was synthesized using High-Capacity cDNA Archive Kit (Applied Biosystems, Weiterstadt, Germany). For gene expression assays, cDNA was amplified using multiplex real-time PCR reactions on a StepOne Plus (Applied Biosystems) [5].

TaqMan primers and probes were derived from the commercially available TaqMans® Gene Expression Assays (Applied Biosystems) (Supporting Information Table 1). Relative changes in gene expression levels were determined using the $2^{-\Delta\Delta Ct}$ method. The cycle number at which the transcripts were detectable (C_t) was normalized to the cycle number of glyceraldehyde-3-phosphate dehydrogenase (GAPDH) detection, referred to as ΔC_t. PCR efficiency was determined by TaqMan analysis on a standard curve for targets and endogenous control amplifications that were highly similar.

2.9. Western Blot

Protein extraction and western blotting were performed as described [20] using rabbit polyclonal antibodies against phospho-AKT (Ser 473) (Santa Cruz Biotechnology) and AKT (Santa Cruz Biotechnology). Bound primary antibody was detected with HRP (horseradish peroxidase)-conjugated anti-rabbit antibody (DAKO, Glostrup, Denmark), and blots were developed using an enhanced chemiluminescence detection system (ECL kit, Amersham Pharmacia, Uppsala, Sweden). The density of the specific bands was quantified with an imaging densitometer (Scion Image, Frederick, MD, USA).

2.10. Statistical analysis

Results are expressed as the mean ± SEM. Significant differences were evaluated by one way analysis of variance (ANOVA) and Newman–Keul's test. $P < 0.05$ was considered to be significant for a difference.

3. Results

3.1. Quercetin improves histological and biochemical findings in MCD-fed mice.

There were not significant differences between control groups of every week and between Control and Control Q groups, so we simplified results by representing the average values over the entire period of time corresponding to control group without quercetin administration (CONTROL).

Supporting Information Table 2 shows the evolution of body and liver weights of mice fed with control, MCD or MCD supplemented with quercetin diets. As previously described [21,22], MCD-fed mice showed a significant reduction in body and liver weights in comparison with the control group, which were not modified by quercetin treatment.

As shown in Fig. 1A, administration of the MCD diet resulted in a classical pathophysiological picture of NASH, with microvesicular and macrovesicular steatosis, indicative of disturbed lipid metabolism, and multiple foci of inflammatory cell accumulations in the liver. Histopathological evaluations revealed that treatment with quercetin resulted in reduced NAFLD activity score (steatosis, inflammation, and ballooning) (Fig.1B).

Dietary MCD feeding caused a marked and progressive elevation of plasma ALT and AST activities, indicating considerable hepatocellular injury, whereas plasma glucose, triglyceride, HDL, LDL and cholesterol concentrations were reduced in comparison with controls. In addition, plasma albumin levels remained unaffected by the MCD diet. Quercetin supplementation significantly decreased plasma ALT levels, and increased plasma glucose and TG levels compared to MCD-fed mice by the fourth week of treatment (Supporting Information Table 3).

3.2. Quercetin decreases NAFLD-associated lipid accumulation and lipoperoxidation in the MCD model of fatty liver.

Oil Red O and Bodipy 493/503 stainings, exhibited in Fig. 2A-B, revealed a significant induction of liver lipid accumulation in MCD-fed mice compared to control mice, increasing with the progression of the disease. Lipid droplets predominantly concentrated in zone 1 (periportal), notably in the first weeks, when lipid droplet size appeared to be larger. Quercetin treatment reduced steatosis and seemed to influence lipid droplet size as shown in representative images of fourth week (Fig. 2A-B), displaying in the liver less but larger lipid droplets than those from non quercetin-treated MCD-fed mice. These results were correlated with liver triglyceride (TG) and free fatty acid (FFA) contents that were enhanced in MCD group compared with control mice, and reduced by quercetin (Fig. 2C).

Lipid peroxidation, visualized by Bodipy 581/591 C_{11} staining, was markedly higher in MCD group compared to control mice. Noteworthy, this increase was greater in the first weeks. Unlike steatosis, lipoperoxidation was characteristically predominant in the intralobular region around the central vein and quercetin was also able to reduce it, mainly by the fourth week of treatment (Fig. 2B).

3.3. Quercetin reduces lipoperoxidation by regulating inflammatory and oxidative/nitrosative stress-related genes in the MCD model of fatty liver.

To investigate the contribution of the quercetin antioxidant and antiinflammatory capacities to the reduction of lipid peroxidation we assessed the effect of this flavonoid on mRNA levels of tumor necrosis factor (TNF)α, osteopontin (OPN), suppressor of cytokine signaling (SOCS)3 and inducible nitric oxide synthase (iNOS).

As shown in Fig. 3, MCD feeding caused a significant upregulation of these genes that was effectively attenuated by quercetin.

3.4. Quercetin reduces lipid accumulation by modulating lipid metabolism-related gene expression in the MCD model of fatty liver.

To examine the contribution of lipid metabolism gene expression modulation to the reduction of lipid accumulation by quercetin we assessed the effect of quercetin on mRNA levels of *de novo* lipogenesis genes liver X receptor (LXR)α and sterol regulatory element binding protein (SREBP)-1c, fatty acid uptake- and trafficking-related genes FAT/CD36, FABP1 and fatty acid transport protein (FATP)5, and the trancription factors forkhead box protein (FOX)A1, peroxisome proliferator-activated receptor (PPAR)α, CCAAT/enhancer binding protein (C/EBP)α, C/EBPβ and small heterodimer partner (SHP) (Fig. 4 and 5).

We observed an early slight induction of LXRα and SREBP-1c gene expression in MCD-fed mice compared to control mice (LXRα, 2W: +14%; SREBP-1c, 2W: +18%) that was reduced by quercetin treatment (LXRα, 2W: -8%; SREBP-1c, 2W: -12% *vs* MCD group).

Nevertheless, it is worthy of mention the significant progressive upregulation of FAT/CD36 expression observed in mice fed with MCD diet that was partially attenuated after quercetin treatment (Fig. 4A). Moreover, examination of representative immunofluorescence images of third week revealed a main cytoplasmic membrane distribution of FAT/CD36 protein in control mice, whose levels where increased by MCD feeding not only in cytoplasmic membrane but also in cytosol and around nucleus and lipid droplets, and reduced by quercetin (Fig. 4B). As shown in Fig. 4A, we also found a significant reduction of FABP1 and FATP5 expression in MCD-fed mice compared with control mice and quercetin was able to slightly attenuate this reduction.

Regarding transcription factors previously reported to be regulators of fatty acid uptake- and trafficking-related genes we observed their expressions reduced in mice fed with

MCD diet compared to control mice. This effect was also observed in SHP expression, unlike C/EBPβ expression that was progressively induced. Quercetin was able to increase the expression of most MCD-downregulated genes and reduce C/EBPβ overexpression by fourth week of treatment (Fig. 5).

3.5. Quercetin modulates oxidative/nitrosative stress, inflammation, and lipid metabolism in MCD-treated Huh7 cells.

Given the results obtained in our *in vivo* model, we proposed to investigate the mechanisms involved in the modulatory effect of quercetin on NAFLD development in an *in vitro* model. Huh7 cells were incubated with MCD medium alone or combined with quercetin 10 μM for 24 hours and antioxidant and antiinflammatory capacities and lipid accumulation inhibition by quercetin were tested. No significant differences between results obtained from Control and Control Q groups were observed, thereby a single control group (control group without quercetin treatment) was shown in order to simplify the representation of the results. Analysis of fluorescence microscopy images shown in Fig. 6 revealed an increase of fatty acid uptake by Huh7 cells after 24 hours of MCD treatment that was markedly attenuated by quercetin, which was correlated with FAT/CD36 gene expression modulation. FABP1 and FATP5 were downregulated in MCD-treated Huh7 compared with control cells and their expression was slightly increased by quercetin (Fig. 7A). Regarding transcription factors (Fig. 7B), MCD medium caused a reduction of FOXA1, PPARα, and C/EBPα expression, showing quercetin an opposite effect. On the contrary, SHP and C/EBPβ were upregulated in MCD-treated cells and quercetin was able to slightly diminish this upregulation. Regarding to *de novo* lipogenesis, as we observed *in vivo*, MCD medium induced a significant increase of LXRα and SREBP-1c gene expression (LXRα: +35%; SREBP-1c: +102%) that was reverted by quercetin, there

being not significant differences *vs* Huh7 control in LXRα expression (LXRα: -24%, *vs* MCD-treated cells).

As shown in Fig. 7C, Bodipy 493/503 and Bodipy 581/591 C_{11} stainings revealed an increase of cytoplasmic lipids (green) and lipid peroxidation (red), respectively, induced by MCD medium that was reduced by quercetin treatment. This is in agreement with RT-qPCR results obtained regarding mRNA expression of inflammatory and oxidative/nitrosative stress-related genes after MCD treatment, significantly downregulated by quercetin (Fig. 7D). Lipoperoxidation induction in addition to ROS/RNS production were confirmed by flow cytometry in MCD-treated cells (Fig. 7E).

3.6. Modulation of PI3K/AKT pathway activation in MCD-fed mice and MCD-treated Huh7 cells by quercetin contributes to its antioxidative, antiinflammatory and antilipogenic effects.

In order to investigate the role of PI3K/AKT in NAFLD pathogenesis and the effect of quercetin on this signalling pathway, we assessed its activation through phosphorylation levels of AKT in MCD and MCD Q-fed mice. MCD feeding caused a progressive increase of AKT phosphorylation and quercetin was able to attenuate this increase, notably at second week of treatment (Fig. 8A).

Proven the activation of PI3K/AKT pathway by MCD diet and the inhibitory effect of quercetin in mice, we also assessed AKT activation in MCD-treated Huh7 cells and the effect of PI3K inhibition with LY294002 and/or quercetin in the expression of all studied genes. As shown in Fig. 8B, PI3K/AKT pathway was activated in MCD-treated cells and inhibited by LY294002 and quercetin. As shown in microscopy fluorescence images of Fig. 7C, PI3K/AKT pathway inhibition induced a reduction in lipid droplets

content while lipoperoxidation seemed to be diminished only by quercetin treatment, as confirmed by flow cytometry (Fig. 7E).

Moreover, most of studied genes were upregulated by PI3K/AKT activation as demonstrated by the reduction of their expression after LY294002 treatment. Nevertheless, iNOS, FATP5, PPARα and C/EBPα appeared to be downregulated by this pathway as shown by their overexpression after LY294002 treatment. Treatment with quercetin did not cause significant alterations in gene expression of most studied genes when PI3K/AKT was inhibited by LY294002. Only iNOS, FABP1 and FAT/CD36 gene expression showed significant differences when LY294002 combined with quercetin compared with LY294002 treatment alone (Fig. 7A, B and D).

4. Discussion

NAFLD is associated with a higher risk of death from cardiovascular and liver-related complications [23]. Currently available drugs proposed for NAFLD treatment have been reported to present poor efficacy and safety [24], so it is necessary to investigate the molecular mechanisms implicated in the establishment and progression of the disease as target for new therapies. Here we show for the first time the relationship between inflammation, nitrosative/oxidative stress and lipid metabolism-related pathways alteration implicated in NAFLD development and the use of quercetin as a potential strategy for NAFLD treatment focused on its capacity to counteract gene expression deregulation associated to these pathways.

Methionine and choline deficiency is the classical dietary model for the study of NASH. This diet induces steatohepatitis rapidly in rodents and male C57BL/6 mice develop the histological features that most closely resemble those seen in human NASH compared with other models [25]. MCD-fed mice in our study displayed classical biochemical parameter

alterations of this model, as well as a prominent hepatic steatosis predominantly in zone 1 [26], and marked inflammation forming intralobular foci.

Furthermore, MCD-related steatosis progressed from macrosteatosis to microsteatosis, allowing the increased surface area of small lipid droplets a high grade of peroxidizability, as previously described [27]. In this regard, we found that quercetin was able to reduce the number and increase the size of lipid droplets, leading to a less susceptibility of fatty acids to peroxidation, which was associated with reduced FFA and TG contents, as previously reported in nutritional models of NAFLD in C57B/6J mice [28].

On the other hand, higher degree of lipoperoxidation in MCD-fed mice was associated with an enhanced inflammatory and oxidative/nitrosative stress-related gene expression, responsible for inflammation in addition to RNS and ROS production typical of NAFLD [11,17,29,30]. As expected, quercetin was able to attenuate this gene expression alteration because of its well-known anti-inflammatory and antioxidant capacities [11,12,31-33].

In spite of the implication of *de novo* lipogenesis deregulation in NAFLD [30,34, 35-38], fatty acid uptake seems to play a key role in the pathogenesis of this disease [5]. In our *in vivo* model, we found low FAT/CD36 levels in control mice, distributed in the cytoplasmic membrane unlike the high levels observed in MCD mice, with an enhanced content not only in plasma membrane, but also in cytosol, around lipid droplets and perinuclear region, likely endoplasmic reticulum [39,40], which associated with an increased hepatic FAT/CD36 translational efficiency, as previously reported under inflammatory stress [41,42]. Moreover, FATP5 seems to present a tendency to diminish its expression in NAFLD patients with the progression of the disease [43], in agreement with our results even though other authors have reported a reversion of diet-induced

NAFLD by silencing FATP5 [44]. Regarding to FABP1, it has already been reported to be repressed in both NAFLD *in vivo* models and patients [6], as confirmed in the present study. FABP1 and FATP5 downregulation was slightly attenuated by the treatment with quercetin, nevertheless FAT/CD36 protein and mRNA increased levels were significantly reduced by this flavonol, as previously observed in HFD models [28,45].

It has been reported that some natural compounds are able to reduce MCD-induced C/EBPβ upregulation, which is associated with a greater ROS production [37,46]. Moreover, it has been demonstrated that C/EBPβ overexpression increases protein and mRNA levels of FAT/CD36 which explains, at least in part, the results obtained in our *in vivo* and *in vitro* MCD models [47]. ROS/RNS production, iNOS expression and NF-κB activation appear to be responsible for PPARα downregulation and subsequent lipid accumulation [48], and quercetin reduces its inhibition [11]. This is in accordance with our study, as we found a deep downregulation of PPARα in both *in vivo* and *in vitro* models of NAFLD, attenuated by quercetin treatment. This downregulation correlated with impaired FATP5 and FABP1 expressions, that in fact are activated by PPARα in the liver [6,49]. Regarding to FOXA1, also activator of FABP1 [6], displayed a similar expression and response to quercetin to that exhibited by PPARα.

SHP is an orphan nuclear receptor whose upregulation is associated with an increased neutral lipid accumulation that characterizes the state of steatosis [50]. Nevertheless, the increase in free fatty acids content could repress SHP activation [51], contributing to increased inflammation and progression of the disease from simple steatosis to steatohepatitis [35,52]. Although it has been described that SHP seems to be a FAT/CD36 activator [53] and despite SHP upregulation in MCD-treated cells and MCD-fed mice at first week (data not shown), it shows a tendency towards

downregulation as previously observed in MCD-fed mice [35]. Therefore, SHP does not appear to play any role in the NAFLD-associated FAT/CD36 increase, at least in later stages of the disease. Indeed, quercetin was able to induce SHP expression in our *in vivo* model, as observed in other studies after procyanidins administration displaying a plasma triglyceride-lowering effect [54].

As we have previously reported, PI3K/AKT pathway activation was involved in hepatitis C virus-associated steatosis development [55]. It has already been described the activation of this pathway in patients with NAFLD [56] and in cell culture after MCD medium treatment [17], in agreement with our results. Given the implication of the PI3K/AKT pathway in the pathogenesis of NAFLD, we aimed to investigate the role of its activation in the deregulation of gene expression observed in our MCD models. Chemical inhibition of AKT phosphorylation by LY294002 in MCD-treated cells revealed that most of studied genes were upregulated through AKT activation. Previous studies have already shown an attenuated transcription of TNFα and FAT/CD36 after LY294002 treatment in macrophages [57,58]. Nevertheless, FABP1 and FOXA1 were downregulated in MCD-treated cells when the PI3K/AKT pathway is activated, so the inhibition exerted by other via seems to be dominant *vs* PI3K/AKT activation for their regulation. This can also explain SHP downregulation since the second week of MCD feeding in mice. On the contrary, FATP5, PPARα and C/EBPα were overexpressed after LY294002 treatment, what is in accordance with the repression of these genes in MCD groups when the PI3K/AKT pathway is activated. Regarding to C/EBPα, several studies have already shown the implication of PI3K/AKT activation in its repression, in agreement with our results [59-61]. Surprisingly, despite its induction in MCD-treated cells and mice, iNOS gene expression was very repressed by this pathway activation, as previously observed in macrophages [62].

Recently, we showed that the modulatory effect of quercetin on HCV-induced liver steatosis development involved oxidative/nitrosative stress blockage and subsequent inactivation of the PI3K/AKT pathway [12]. A similar mechanism underlies the modulatory effect of quercetin in gene expression observed in our NAFLD models. This is in agreement with the lack of effect of quercetin on SOCS3, TNFα, C/EBPβ, FATP5, PPARα and C/EBPα expression beyond LY294002 treatment, when the PI3K/AKT pathway is greatly inhibited by this chemical inhibitor. In this regard, it has been recently reported the activation of C/EBPβ by AKT phosphorylation and its downregulation and suppression of AKT phosphorylation after a treatment with the flavonoid baicalin in adipocytes [63], as we observed in the quercetin treated groups of our study. On the contrary, this flavonoid exerted its modulatory effect on gene expression by other pathway different from PI3K/AKT inactivation in the case of FABP1, FOXA1, and iNOS, since treatment with quercetin produces an opposite effect on their expression from what was expected by the inhibition of PI3K activity.

When MCD-treated cells were incubated with quercetin, SHP and FAT/CD36 were downregulated, in agreement with expected because of the PI3K/AKT pathway blockage. Nevertheless, in MCD-fed mice, this flavonol ameliorated SHP downregulation and was able to increase FAT/CD36 expression in MCD LY-treated cells, demonstrating another pathway of action. Some authors have reported an induction of sirtuin 1 (Sirt1) and nuclear factor E2-related factor 2 (Nrf2) expressions by quercetin [11,32], which could contribute to its effect, at least on inflammation and nitrosative/oxidative stress-related genes, beyond PI3K/AKT pathway modulation, as it has been also described recently for apigenin and luteolin treatments *in vitro* [64]. Moreover, downregulation of PI3K/AKT pathway by quercetin contributes to diminish

lipid accumulation through repressing FAT/CD36 translocation to the plasma membrane [65].

Overall, in our study oxidative/nitrosative stress, inflammation and lipid metabolism-related genes displayed a tendency to normalize by quercetin treatment in both *in vivo* and *in vitro* models of NAFLD. This modulatory effect of quercetin is mediated at least in part through PI3K/AKT pathway inactivation, being also implicated other mechanisms that need to be further investigated (Fig. 9). These results place quercetin as a potential therapeutic strategy for preventing the progression of NAFLD by counteracting gene expression deregulation associated to this common chronic liver disorder.

Acknowledgments

This work was supported by grants to Javier González-Gallego and Sonia Sánchez Campos from Ministerio de Economía y Competitividad/FEDER (BFU2013-48141-R), Javier González Gallego and José Luis Olcoz from Junta de Castilla y León (LE135U13 and GRS1000/A/14, respectively), and Ramiro Jover from Fondo de Investigación Sanitaria (FIS), Instituto de Salud Carlos III (PI10/00194). María V. García-Mediavilla and Marta Benet were supported by CIBERehd contracts. CIBERehd is funded by the Instituto de Salud Carlos III, Spain.

The authors declare no conflict of interest.

5. References

[1] Machado, M., Cortez-Pinto, H., Non-alcoholic steatohepatitis and metabolic syndrome. *Curr. Opin. Clin. Nutr. Metab. Care*. 2006*, 9*, 637-642.

[2] Tiniakos, D.G., Vos, M.B., Brunt, E.M., Nonalcoholic fatty liver disease: pathology and pathogenesis. *Annu. Rev. Pathol.* 2010*, 5*, 145-171.

[3] Koo, S.H., Nonalcoholic fatty liver disease: molecular mechanisms for the hepatic steatosis. *Clin. Mol. Hepatol.* 2013*, 19*, 210-215.

[4] Neuschwander-Tetri, B.A., Nontriglyceride hepatic lipotoxicity: the new paradigm for the pathogenesis of NASH. *Curr. Gastroenterol. Rep.* 2010*, 12*, 49-56.

[5] Miquilena-Colina, M.E., Lima-Cabello, E., Sánchez-Campos, S., García-Mediavilla, M.V.*, et al.*, Hepatic fatty acid translocase CD36 upregulation is associated with insulin resistance, hyperinsulinaemia and increased steatosis in non-alcoholic steatohepatitis and chronic hepatitis C. *Gut*. 2011*, 60*, 1394-1402.

[6] Guzmán, C., Benet, M., Pisonero-Vaquero, S., Moya, M.*, et al.*, The human liver fatty acid binding protein (FABP1) gene is activated by FOXA1 and PPARalpha; and repressed by C/EBPalpha: Implications in FABP1 down-regulation in nonalcoholic fatty liver disease. *Biochim. Biophys. Acta*. 2013*, 1831*, 803-818.

[7] Torres, D.M., Harrison, S.A., Diagnosis and therapy of nonalcoholic steatohepatitis. *Gastroenterology*. 2008*, 134*, 1682-1698.

[8] Zeng, C.H., Zeng, P., Deng, Y.H., Shen, N.*, et al.*, The effects of curcumin derivative on experimental steatohepatitis. *Zhonghua Gan Zang Bing Za Zhi*. 2011*, 19*, 454-459.

[9] Salamone, F., Galvano, F., Cappello, F., Mangiameli, A.*, et al.*, Silibinin modulates lipid homeostasis and inhibits nuclear factor kappa B activation in experimental nonalcoholic steatohepatitis. *Transl. Res.* 2012*, 159*, 477-486.

[10] González-Gallego, J., García-Mediavilla, M.V., Sánchez-Campos, S., Tuñón, M.J., Fruit polyphenols, immunity and inflammation. *Br. J. Nutr.* 2010*, 104 Suppl 3*, S15-27.

[11] Ying, H.Z., Liu, Y.H., Yu, B., Wang, Z.Y.*, et al.*, Dietary quercetin ameliorates nonalcoholic steatohepatitis induced by a high-fat diet in gerbils. *Food Chem. Toxicol.* 2013*, 52*, 53-60.

[12] Pisonero-Vaquero, S., García-Mediavilla, M.V., Jorquera, F., Majano, P.L.*, et al.*, Modulation of PI3K-LXRalpha-dependent lipogenesis mediated by oxidative/nitrosative stress contributes to inhibition of HCV replication by quercetin. *Lab. Invest.* 2014*, 94*, 262-274.

[13] Li, X., Wang, R., Zhou, N., Wang, X.*, et al.*, Quercetin improves insulin resistance and hepatic lipid accumulation in a NAFLD cell model. *Biomed. Rep.* 2013*, 1*, 71-76.

[14] Vidyashankar, S., Sandeep Varma, R., Patki, P.S., Quercetin ameliorate insulin resistance and up-regulates cellular antioxidants during oleic acid induced hepatic steatosis in HepG2 cells. *Toxicol. In. Vitro.* 2013*, 27*, 945-953.

[15] Kleiner, D.E., Brunt, E.M., Van Natta, M., Behling, C.*, et al.*, Design and validation of a histological scoring system for nonalcoholic fatty liver disease. *Hepatology*. 2005*, 41*, 1313-1321.

[16] Gupta, N.A., Mells, J., Dunham, R.M., Grakoui, A.*, et al.*, Glucagon-like peptide-1 receptor is present on human hepatocytes and has a direct role in decreasing hepatic steatosis in vitro by modulating elements of the insulin signaling pathway. *Hepatology*. 2010*, 51*, 1584-1592.

[17] Sahai, A., Pan, X., Paul, R., Malladi, P.*, et al.*, Roles of phosphatidylinositol 3-kinase and osteopontin in steatosis and aminotransferase release by hepatocytes treated with methionine-choline-deficient medium. *Am. J. Physiol. Gastrointest. Liver Physiol.* 2006*, 291*, G55-62.

[18] Crespo, I., García-Mediavilla, M.V., Gutiérrez, B., Sánchez-Campos, S., *et al.*, A comparison of the effects of kaempferol and quercetin on cytokine-induced pro-inflammatory status of cultured human endothelial cells. *Br. J. Nutr.* 2008, *100*, 968-976.

[19] Dionisio, N., García-Mediavilla, M.V., Sánchez-Campos, S., Majano, P.L., *et al.*, Hepatitis C virus NS5A and core proteins induce oxidative stress-mediated calcium signalling alterations in hepatocytes. *J. Hepatol.* 2009, *50*, 872-882.

[20] Kretzmann, N.A., Fillmann, H., Mauriz, J.L., Marroni, C.A., *et al.*, Effects of glutamine on proinflammatory gene expression and activation of nuclear factor kappa B and signal transducers and activators of transcription in TNBS-induced colitis. *Inflamm. Bowel Dis.* 2008, *14*, 1504-1513.

[21] Leclercq, I.A., Farrell, G.C., Field, J., Bell, D.R., *et al.*, CYP2E1 and CYP4A as microsomal catalysts of lipid peroxides in murine nonalcoholic steatohepatitis. *J. Clin. Invest.* 2000, *105*, 1067-1075.

[22] Ip, E., Farrell, G.C., Robertson, G., Hall, P., *et al.*, Central role of PPARalpha-dependent hepatic lipid turnover in dietary steatohepatitis in mice. *Hepatology*. 2003, *38*, 123-132.

[23] Ekstedt, M., Hagstrom, H., Nasr, P., Fredrikson, M., *et al.*, Fibrosis stage is the strongest predictor for disease-specific mortality in NAFLD after up to 33 years of follow-up. *Hepatology*. 2014.

[24] Musso, G., Gambino, R., Cassader, M., Pagano, G., A meta-analysis of randomized trials for the treatment of nonalcoholic fatty liver disease. *Hepatology*. 2010, *52*, 79-104.

[25] Almonacid-Urrego, C.C., Sánchez-Campos, S., Tuñón, M.J., González-Gallego, J., Non-alcoholic steatohepatitis: what can we learn from animal models?. *Curr. Med. Chem.* 2012*, 19*, 1389-1404.

[26] Takahashi, Y., Soejima, Y., Fukusato, T., Animal models of nonalcoholic fatty liver disease/nonalcoholic steatohepatitis. *World J. Gastroenterol.* 2012*, 18*, 2300-2308.

[27] Ronis, M.J., Baumgardner, J.N., Marecki, J.C., Hennings, L.*, et al.*, Dietary fat source alters hepatic gene expression profile and determines the type of liver pathology in rats overfed via total enteral nutrition. *Physiol. Genomics*. 2012*, 44*, 1073-1089.

[28] Jung, C.H., Cho, I., Ahn, J., Jeon, T.I., Ha, T.Y., Quercetin reduces high-fat diet-induced fat accumulation in the liver by regulating lipid metabolism genes. *Phytother. Res.* 2013*, 27*, 139-143.

[29] Zhang, L., Xu, J., Song, H., Yao, Z., Ji, G., Extracts from Salvia-Nelumbinis naturalis alleviate hepatosteatosis via improving hepatic insulin sensitivity. *J. Transl. Med.* 2014*, 12*, 236-014-0236-8.

[30] Lima-Cabello, E., García-Mediavilla, M.V., Miquilena-Colina, M.E., Vargas-Castrillón, J.*, et al.*, Enhanced expression of pro-inflammatory mediators and liver X-receptor-regulated lipogenic genes in non-alcoholic fatty liver disease and hepatitis C. *Clin. Sci. (Lond)*. 2011*, 120*, 239-250.

[31] Marcolin, E., San-Miguel, B., Vallejo, D., Tieppo, J.*, et al.*, Quercetin treatment ameliorates inflammation and fibrosis in mice with nonalcoholic steatohepatitis. *J. Nutr.* 2012*, 142*, 1821-1828.

[32] Panchal, S.K., Poudyal, H., Brown, L., Quercetin ameliorates cardiovascular, hepatic, and metabolic changes in diet-induced metabolic syndrome in rats. *J. Nutr.* 2012*, 142*, 1026-1032.

[33] Crespo, I., García-Mediavilla, M.V., Almar, M., González, P.*, et al.*, Differential effects of dietary flavonoids on reactive oxygen and nitrogen species generation and changes in antioxidant enzyme expression induced by proinflammatory cytokines in Chang Liver cells. *Food Chem. Toxicol.* 2008*, 46*, 1555-1569.

[34] Ameer, F., Scandiuzzi, L., Hasnain, S., Kalbacher, H., Zaidi, N., De novo lipogenesis in health and disease. *Metabolism*. 2014*, 63*, 895-902.

[35] Chanda, D., Lee, C.H., Kim, Y.H., Noh, J.R.*, et al.*, Fenofibrate differentially regulates plasminogen activator inhibitor-1 gene expression via adenosine monophosphate-activated protein kinase-dependent induction of orphan nuclear receptor small heterodimer partner. *Hepatology*. 2009*, 50*, 880-892.

[36] Park, H.S., Jeon, B.H., Woo, S.H., Leem, J.*, et al.*, Time-dependent changes in lipid metabolism in mice with methionine choline deficiency-induced fatty liver disease. *Mol. Cells*. 2011*, 32*, 571-577.

[37] Zhang, X., Shen, J., Man, K., Chu, E.S.*, et al.*, CXCL10 plays a key role as an inflammatory mediator and a non-invasive biomarker of non-alcoholic steatohepatitis. *J. Hepatol.* 2014.

[38] Wang, W., Wang, C., Ding, X.Q., Pan, Y.*, et al.*, Quercetin and allopurinol reduce liver thioredoxin-interacting protein to alleviate inflammation and lipid accumulation in diabetic rats. *Br. J. Pharmacol.* 2013*, 169*, 1352-1371.

[39] Su, X., Abumrad, N.A., Cellular fatty acid uptake: a pathway under construction. *Trends Endocrinol. Metab.* 2009*, 20*, 72-77.

[40] Eyre, N.S., Cleland, L.G., Tandon, N.N., Mayrhofer, G., Importance of the carboxyl terminus of FAT/CD36 for plasma membrane localization and function in long-chain fatty acid uptake. *J. Lipid Res.* 2007*, 48*, 528-542.

[41] Wang, C., Hu, L., Zhao, L., Yang, P., *et al.*, Inflammatory stress increases hepatic CD36 translational efficiency via activation of the mTOR signalling pathway. *PLoS One*. 2014, *9*, e103071.

[42] Luo, Z.L., Tang, L.J., Wang, T., Dai, R.W., *et al.*, Effects of treatment with hydrogen sulfide on methionine-choline deficient diet-induced non-alcoholic steatohepatitis in rats. *J. Gastroenterol. Hepatol.* 2014, *29*, 215-222.

[43] Mitsuyoshi, H., Yasui, K., Harano, Y., Endo, M., *et al.*, Analysis of hepatic genes involved in the metabolism of fatty acids and iron in nonalcoholic fatty liver disease. *Hepatol. Res.* 2009, *39*, 366-373.

[44] Doege, H., Grimm, D., Falcon, A., Tsang, B., *et al.*, Silencing of hepatic fatty acid transporter protein 5 in vivo reverses diet-induced non-alcoholic fatty liver disease and improves hyperglycemia. *J. Biol. Chem.* 2008, *283*, 22186-22192.

[45] Ding, L., Liu, J.L., Hassan, W., Wang, L.L., *et al.*, Lipid modulatory activities of Cichorium glandulosum Boiss et Huet are mediated by multiple components within hepatocytes. *Sci. Rep.* 2014, *4*, 4715.

[46] Shen, B., Yu, J., Wang, S., Chu, E.S., *et al.*, Phyllanthus urinaria ameliorates the severity of nutritional steatohepatitis both in vitro and in vivo. *Hepatology*. 2008, *47*, 473-483.

[47] Qiao, L., Zou, C., Shao, P., Schaack, J., *et al.*, Transcriptional regulation of fatty acid translocase/CD36 expression by CCAAT/enhancer-binding protein alpha. *J. Biol. Chem.* 2008, *283*, 8788-8795.

[48] Cabrero, A., Alegret, M., Sanchez, R.M., Adzet, T., *et al.*, Increased reactive oxygen species production down-regulates peroxisome proliferator-activated alpha pathway in C2C12 skeletal muscle cells. *J. Biol. Chem.* 2002, *277*, 10100-10107.

[49] Motojima, K., Passilly, P., Peters, J.M., Gonzalez, F.J., Latruffe, N., Expression of putative fatty acid transporter genes are regulated by peroxisome proliferator-activated receptor alpha and gamma activators in a tissue- and inducer-specific manner. *J. Biol. Chem.* 1998*, 273*, 16710-16714.

[50] Huang, J., Iqbal, J., Saha, P.K., Liu, J.*, et al.*, Molecular characterization of the role of orphan receptor small heterodimer partner in development of fatty liver. *Hepatology*. 2007*, 46*, 147-157.

[51] Bechmann, L.P., Kocabayoglu, P., Sowa, J.P., Sydor, S.*, et al.*, Free fatty acids repress small heterodimer partner (SHP) activation and adiponectin counteracts bile acid-induced liver injury in superobese patients with nonalcoholic steatohepatitis. *Hepatology*. 2013*, 57*, 1394-1406.

[52] Yang, C.S., Yuk, J.M., Kim, J.J., Hwang, J.H.*, et al.*, Small heterodimer partner-targeting therapy inhibits systemic inflammatory responses through mitochondrial uncoupling protein 2. *PLoS One*. 2013*, 8*, e63435.

[53] Trauner, M., A little orphan runs to fat: the orphan receptor small heterodimer partner as a key player in the regulation of hepatic lipid metabolism. *Hepatology*. 2007*, 46*, 1-5.

[54] Del Bas, J.M., Ricketts, M.L., Baiges, I., Quesada, H.*, et al.*, Dietary procyanidins lower triglyceride levels signaling through the nuclear receptor small heterodimer partner. *Mol. Nutr. Food Res.* 2008*, 52*, 1172-1181.

[55] García-Mediavilla, M.V., Pisonero-Vaquero, S., Lima-Cabello, E., Benedicto, I.*, et al.*, Liver X receptor alpha-mediated regulation of lipogenesis by core and NS5A proteins contributes to HCV-induced liver steatosis and HCV replication. *Lab. Invest.* 2012*, 92*, 1191-1202.

[56] Xu, D., Huang, X.D., Yuan, J.P., Wu, J., *et al.*, Impaired activation of phosphatidylinositol 3-kinase by leptin is a novel mechanism of hepatic leptin resistance in NAFLD. *Hepatogastroenterology*. 2011, *58*, 1703-1707.

[57] Kim, S.M., Jang, H., Son, Y., Lee, S.A., *et al.*, 27-hydroxycholesterol induces production of tumor necrosis factor-alpha from macrophages. *Biochem. Biophys. Res. Commun.* 2013, *430*, 454-459.

[58] Rios, F.J., Koga, M.M., Ferracini, M., Jancar, S., Co-stimulation of PAFR and CD36 is required for oxLDL-induced human macrophages activation. *PLoS One*. 2012, *7*, e36632.

[59] Datta, J., Majumder, S., Kutay, H., Motiwala, T., *et al.*, Metallothionein expression is suppressed in primary human hepatocellular carcinomas and is mediated through inactivation of CCAAT/enhancer binding protein alpha by phosphatidylinositol 3-kinase signaling cascade. *Cancer Res.* 2007, *67*, 2736-2746.

[60] Vivanco, I., Sawyers, C.L., The phosphatidylinositol 3-Kinase AKT pathway in human cancer. *Nat. Rev. Cancer.* 2002, *2*, 489-501.

[61] Wang, G.L., Iakova, P., Wilde, M., Awad, S., Timchenko, N.A., Liver tumors escape negative control of proliferation via PI3K/Akt-mediated block of C/EBP alpha growth inhibitory activity. *Genes Dev.* 2004, *18*, 912-925.

[62] Kim, H.S., Park, E.J., Park, S.W., Kim, H.J., Chang, K.C., A tetrahydroisoquinoline alkaloid THI-28 reduces LPS-induced HMGB1 and diminishes organ injury in septic mice through p38 and PI3K/Nrf2/HO-1 signals. *Int. Immunopharmacol.* 2013, *17*, 684-692.

[63] Kwak, D.H., Lee, J.H., Song, K.H., Ma, J.Y., Inhibitory effects of baicalin in the early stage of 3T3-L1 preadipocytes differentiation by down-regulation of PDK1/Akt phosphorylation. *Mol. Cell. Biochem.* 2014, *385*, 257-264.

[64] Bumke-Vogt, C., Osterhoff, M.A., Borchert, A., Guzman-Perez, V.*, et al.*, The Flavones Apigenin and Luteolin Induce FOXO1 Translocation but Inhibit Gluconeogenic and Lipogenic Gene Expression in Human Cells. *PLoS One*. 2014*, 9*, e104321.

[65] Luiken, J.J., Koonen, D.P., Willems, J., Zorzano, A.*, et al.*, Insulin stimulates long-chain fatty acid utilization by rat cardiac myocytes through cellular redistribution of FAT/CD36. *Diabetes*. 2002*, 51*, 3113-3119.

[66] Huang, J., Tabbi-Anneni, I., Gunda, V., Wang, L., Transcription factor Nrf2 regulates SHP and lipogenic gene expression in hepatic lipid metabolism. *Am. J. Physiol. Gastrointest. Liver Physiol.* 2010*, 299*, G1211-21.

[67] Waris, G., Felmlee, D.J., Negro, F., Siddiqui, A., Hepatitis C virus induces proteolytic cleavage of sterol regulatory element binding proteins and stimulates their phosphorylation via oxidative stress. *J. Virol.* 2007*, 81*, 8122-8130.

Figure legends

Fig 1. Effect of MCD diet and quercetin on liver histology in C57BL/6J mice. (A) Photomicrographs of representative liver sections after feeding with MCD or MCD supplemented with quercetin diets for 2, 3 and 4 weeks (W), compared with CONTROL (x100). (B) NAFLD activity score (NAS) (calculated from individual scores for steatosis, lobular inflammation and ballooning). Data are described as the means ± SEM (n=6 mice per group). *P<0.05, **P<0.01, ***P<0.001 *vs* CONTROL; $^{\#}$P<0.05, $^{\#\#}$P<0.01, $^{\#\#\#}$P<0.001 *vs* MCD.

Fig. 2. Effect of quercetin on hepatic lipid accumulation and lipoperoxidation in MCD-fed mice. A) Representative images of Oil Red O-stained liver sections (x100). B) Representative fluorescent images of lipid droplets (Bodipy 493/503, green) and lipoperoxidation (Bodipy 581/591 C_{11}, red) stainings (x100). Nuclei were stained with DAPI (blue). Merged images with green, red and blue fluorescence are also shown. Photographs shown are representative of 6 animals per group. C) Effect of MCD diet and quercetin on hepatic triglyceride and free fatty acid levels. Data are described as the means ± SEM (n=6 mice per group). *P<0.05, **P<0.01, ***P<0.001 *vs* CONTROL; $^{\#}$P<0.05, $^{\#\#}$P<0.01 *vs* MCD.

Fig. 3. Effect of quercetin on inflammatory and oxidative/nitrosative stress-related gene expression in MCD-fed mice. Bar graphs show mRNA levels of TNFα, SOCS3, OPN and iNOS determined by RT-qPCR. Data are described as the means ± SEM (n=6 mice per group). *P<0.05, **P<0.01, ***P<0.001 *vs* CONTROL; $^{\#}$P<0.05, $^{\#\#}$P<0.01, $^{\#\#\#}$P<0.001 *vs* MCD.

Fig 4. Effect of quercetin on fatty acid uptake- and trafficking-related gene expression in MCD-fed mice. A) Representative fluorescent images of FAT/CD36

immunolocalization (red) and lipid droplets staining (Bodipy 493/503, green) at third week (x600). Nuclei were stained with DAPI (blue). Merged images with red, green and blue fluorescence are also shown. White arrows indicate FAT/CD36 localization in cytoplasmic membrane, cytosol and around nucleus and lipid droplets. Photographs shown are representative of 6 mice per group. B) Bar graphs show mRNA levels of FAT/CD36, FABP1 and FATP5 determined by RT-qPCR. Data are described as the means ± SEM of (n=6 mice per group). **P<0.01, ***P<0.001 *vs* CONTROL; $^{\#}$P<0.05, $^{\#\#}$P<0.01, $^{\#\#\#}$P<0.001 *vs* MCD.

Fig. 5. Effect of quercetin on mRNA expression of genes involved in transcriptional regulation of lipid metabolism in MCD-fed mice. Bar graphs show mRNA levels of FOXA1, PPARα, C/EBPα, SHP and C/EBPβ determined by RT-qPCR. Data are described as the means ± SEM of (n=6 mice per group). *P<0.05, **P<0.01, ***P<0.001 *vs* CONTROL; $^{\#}$P<0.05, $^{\#\#}$P<0.01, $^{\#\#\#}$P<0.001 *vs* MCD.

Fig. 6. Effect of quercetin on fatty acid uptake in MCD-treated Huh7 cells. Representative fluorescent images of fatty acid uptake (Bodipy FL C_{12}, green) at 0, 8 and 24 h (x400). Nuclei were stained with DAPI (blue). Merged images with green and blue fluorescence are also shown. Photographs shown are typical results of six independent experiments.

Fig. 7. Effect of quercetin and/or the PI3K-inhibitor LY294002 on lipid metabolism, inflammation, and oxidative/nitrosative stress-related gene expression in MCD-treated cells. Bar graphs show mRNA levels of FAT/CD36, FABP1 and FATP5 (A), iNOS, SOCS3 and TNFα (B), and FOXA1, PPARα, SHP, C/EBPα and C/EBPβ (C), determined by RT-qPCR. D) ROS/RNS production and lipid peroxidation expressed as DCF and Bodipy 581/591 C_{11} fluorescence intensity, respectively, normalized to control

cells (100%). Data are described as the means ± SEM of six independent experiments. *P<0.05, **P<0.01, ***P<0.001 *vs* CONTROL; $^{\#}$P<0.05, $^{\#\#}$P<0.01, $^{\#\#\#}$P<0.001 *vs* MCD; $^{\&\&}$P<0.01, $^{\&\&\&}$P<0.001 MCD Q LY *vs* MCD LY. E) Representative fluorescent images of lipoperoxidation (Bodipy 581/591 C_{11}, red) and lipid droplets (Bodipy 493/503, green) stainings (x400). Nuclei were stained with DAPI (blue). Merged images with red, green and blue fluorescence are also shown. Photographs shown are typical results of six independent experiments.

Fig. 8. Effect of quercetin on PI3K/AKT pathway activation in *in vivo* and *in vitro* MCD models of NAFLD. A) and B) Representative western blot of pAKT (Ser 473) and AKT protein expression in liver from CONTROL, MCD and MCD Q-fed mice and in Huh7 cells incubated with MCD or MCD Q medium alone or combined with the PI3K-inhibitor LY294002, respectively. Densitometry analysis of specific bands expressed as percentage relative to CONTROL (100%). Data are described as the means ± SEM of six independent experiments. **P<0.01, ***P<0.001 *vs* CONTROL; $^{\#\#}$P<0.01, $^{\#\#\#}$P<0.001 *vs* MCD.

Fig. 9. Quercetin counteracts gene expression deregulation associated to NAFLD progression. PI3K/AKT pathway activation in NAFLD triggers the gene expression alteration of FAT/CD36, FATP5, FABP1 and transcription factors implicated in their regulation, in addition to TNFα, SOCS3 and iNOS, leading to an increment of fatty acid uptake and lipotoxicity as well as inflammation and oxidative/nitrosative stress, contributing to NAFLD progression. Quercetin modulates NAFLD-associated gene deregulation by diminishing PI3K/AKT activation, being also implicated other mechanisms that need to be further investigated.

Figure 1

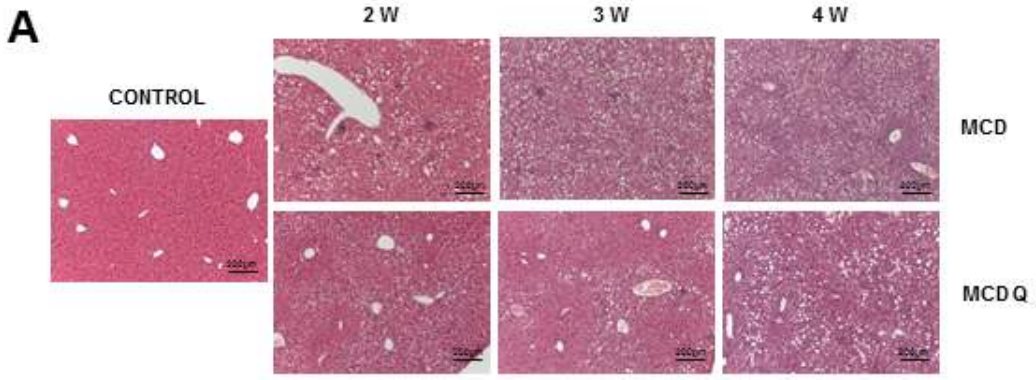
A
2 W
3 W
4 W
CONTROL
MCD
MCD Q

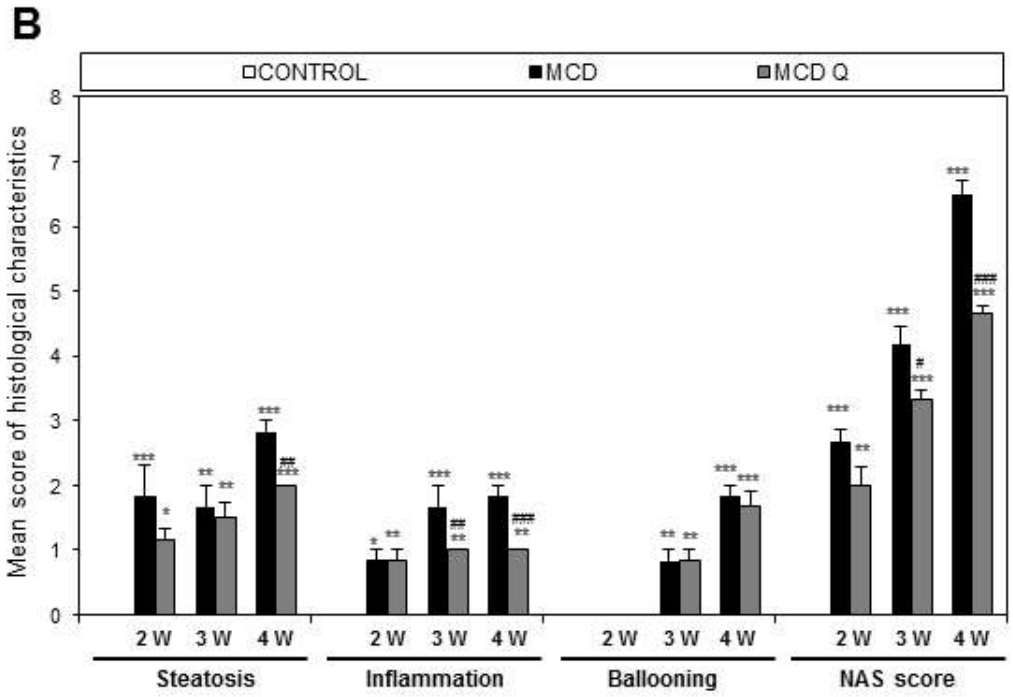
B
CONTROL
MCD
MCD Q
Mean score of histological characteristics
0
1
2
3
4
5
6
7
8
2 W
3 W
4 W
Steatosis
Inflammation
Ballooning
NAS score

Figure 2

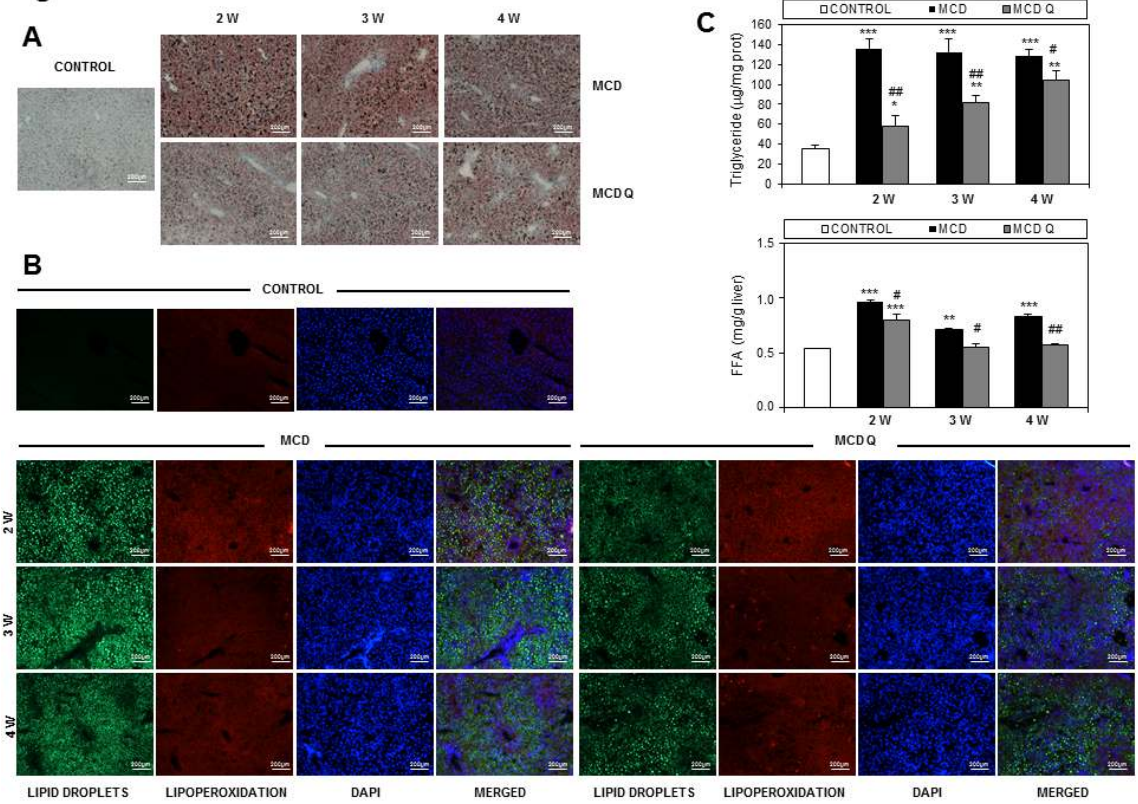
A
2 W
3 W
4 W
CONTROL
MCD
MCD Q
B
CONTROL
MCD
MCD Q
2 W
3 W
4 W
LIPID DROPLETS
LIPOPEROXIDATION
DAPI
MERGED
C
CONTROL
MCD
MCD Q
Triglyceride (µg/mg prot)
FFA (mg/g liver)
2 W
3 W
4 W

Figure 3

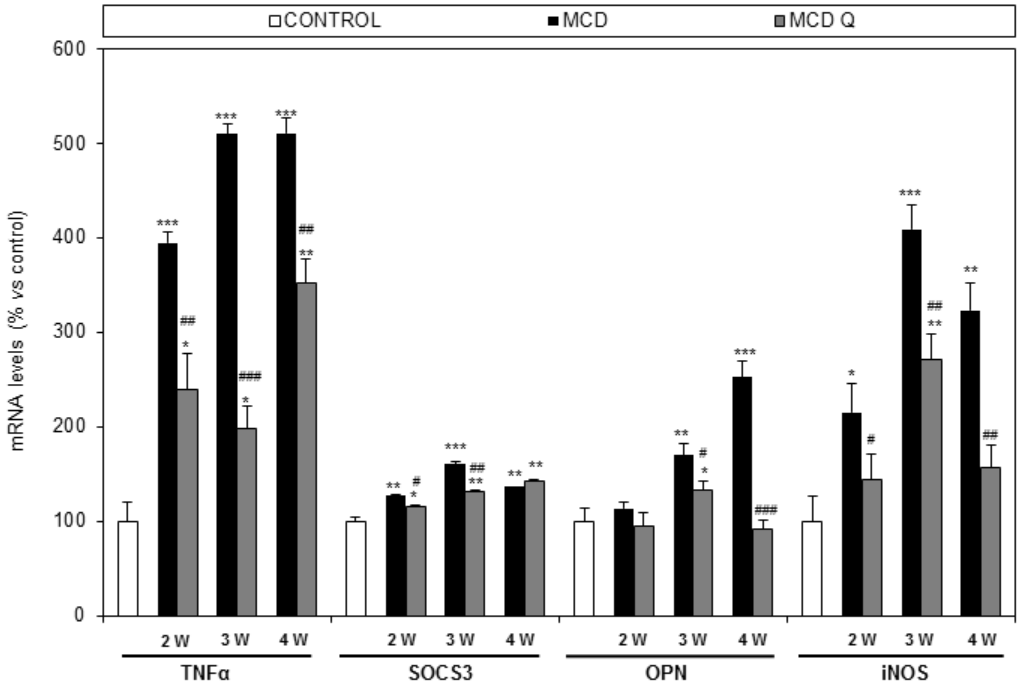
CONTROL
MCD
MCD Q
mRNA levels (% vs control)
600
500
400
300
200
100
0
2 W
3 W
4 W
TNFα
SOCS3
OPN
iNOS

Figure 4

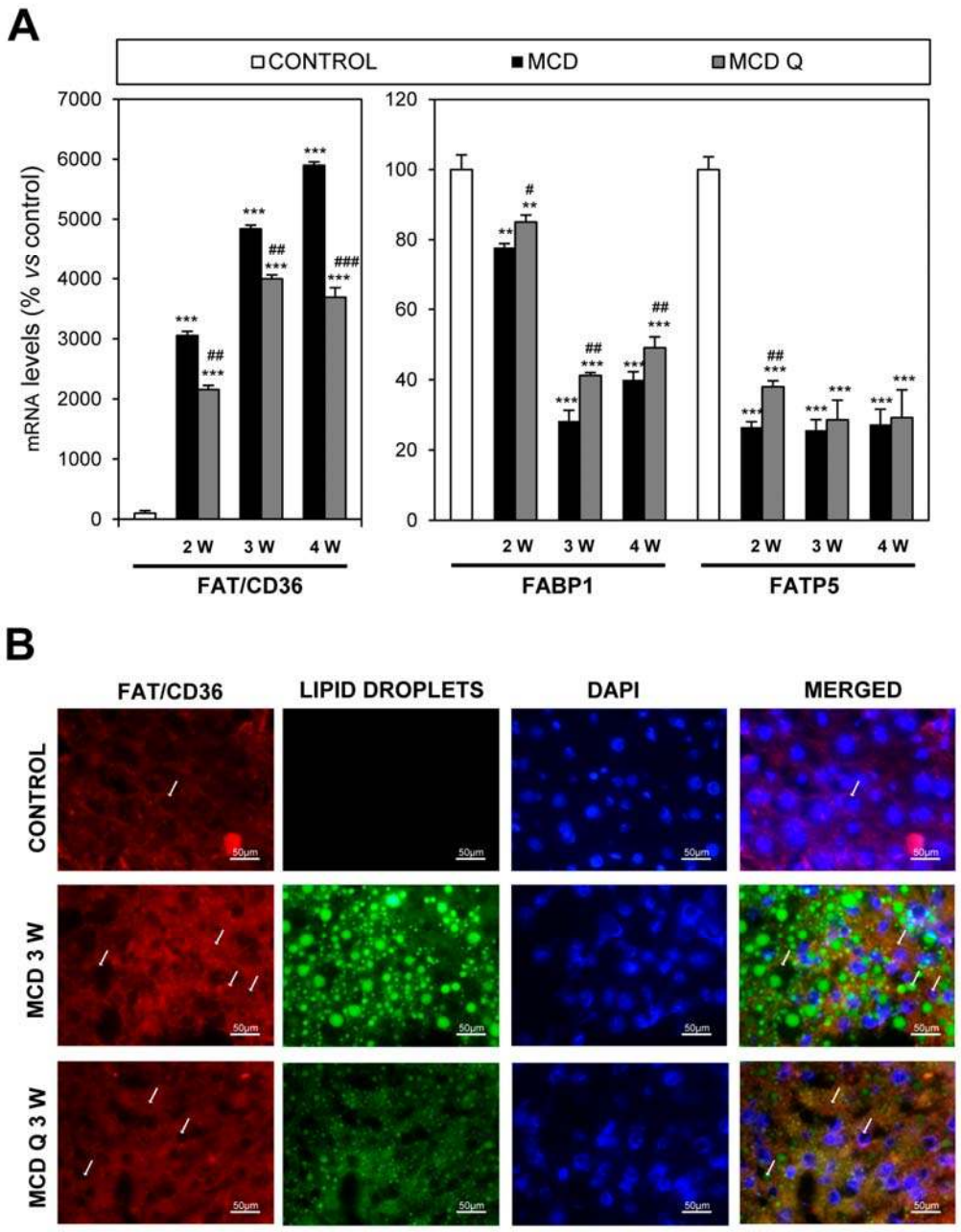
A
CONTROL
MCD
MCD Q
mRNA levels (% vs control)
7000
6000
5000
4000
3000
2000
1000
0
120
100
80
60
40
20
0
2 W
3 W
4 W
FAT/CD36
FABP1
FATP5
B
FAT/CD36
LIPID DROPLETS
DAPI
MERGED
CONTROL
MCD 3 W
MCD Q 3 W
50µm

Figure 5

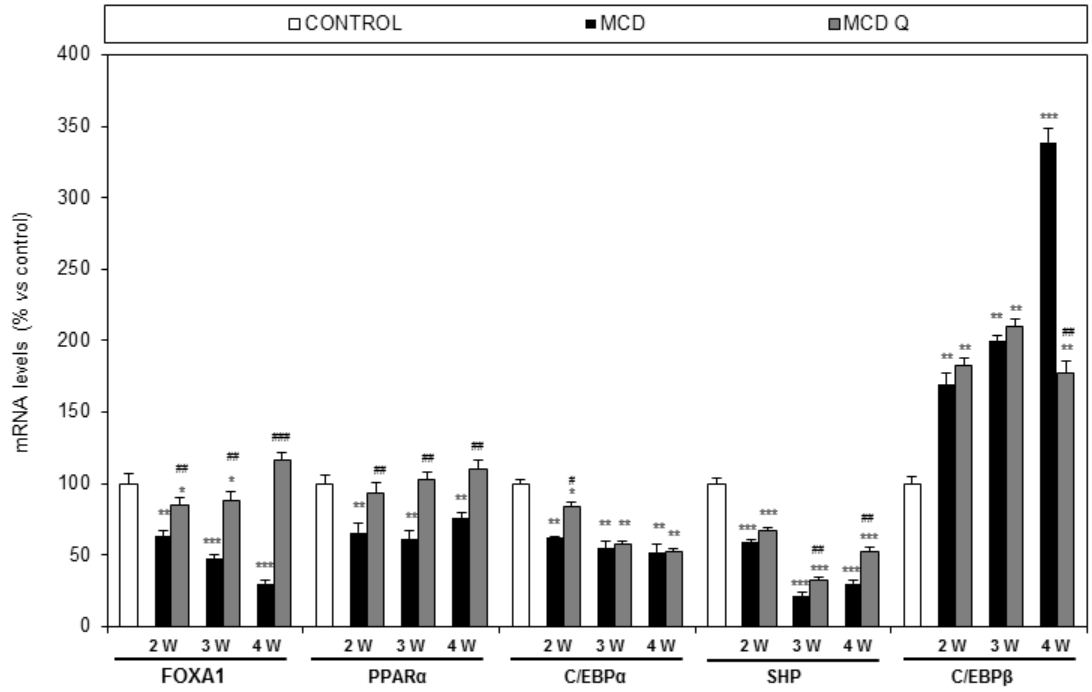
CONTROL
MCD
MCD Q
mRNA levels (% vs control)
400
350
300
250
200
150
100
50
0
2 W
3 W
4 W
FOXA1
PPARα
C/EBPα
SHP
C/EBPβ

Figure 6

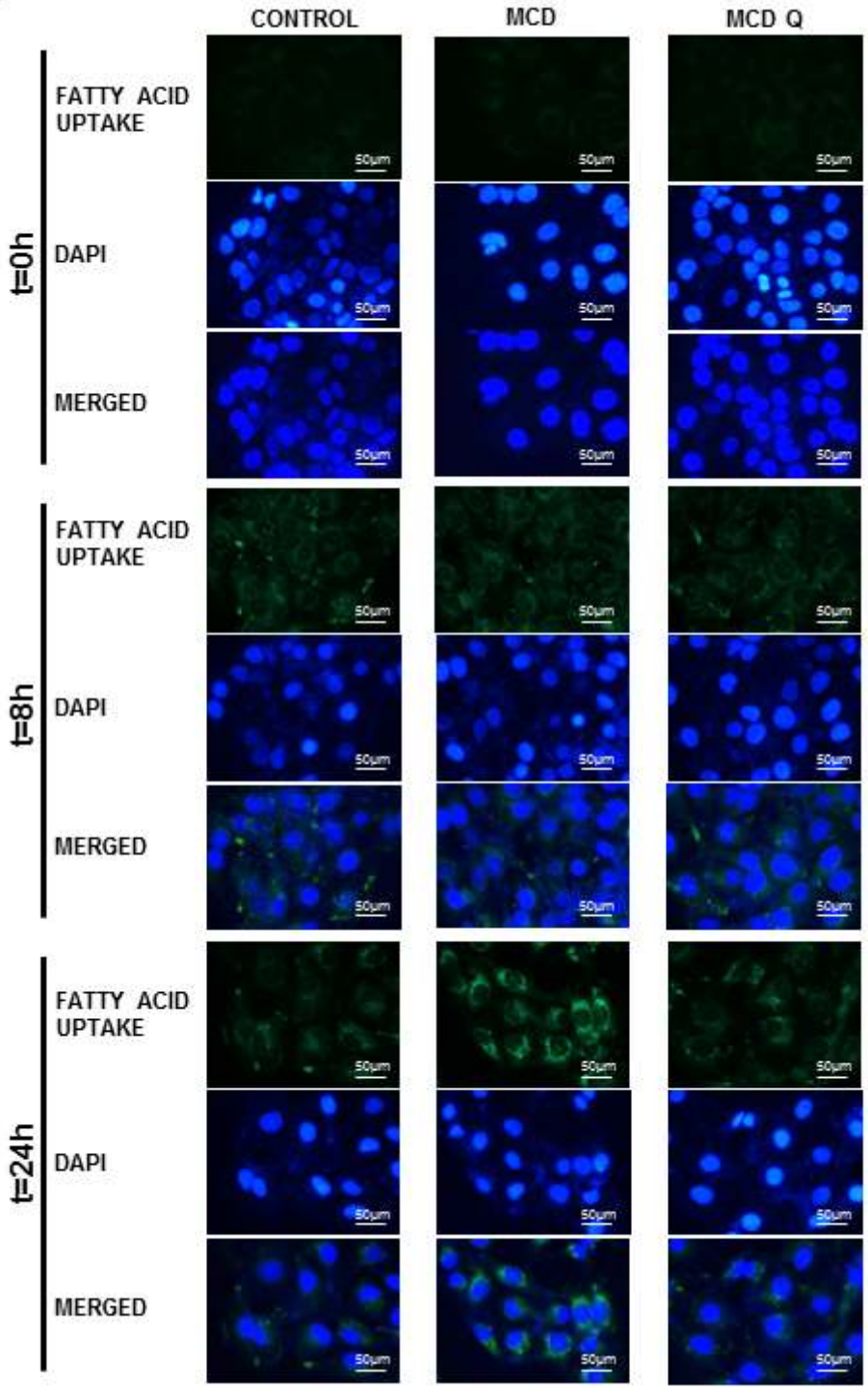
CONTROL
MCD
MCD Q
t=0h
t=8h
t=24h
FATTY ACID UPTAKE
DAPI
MERGED
50µm

Figure 7

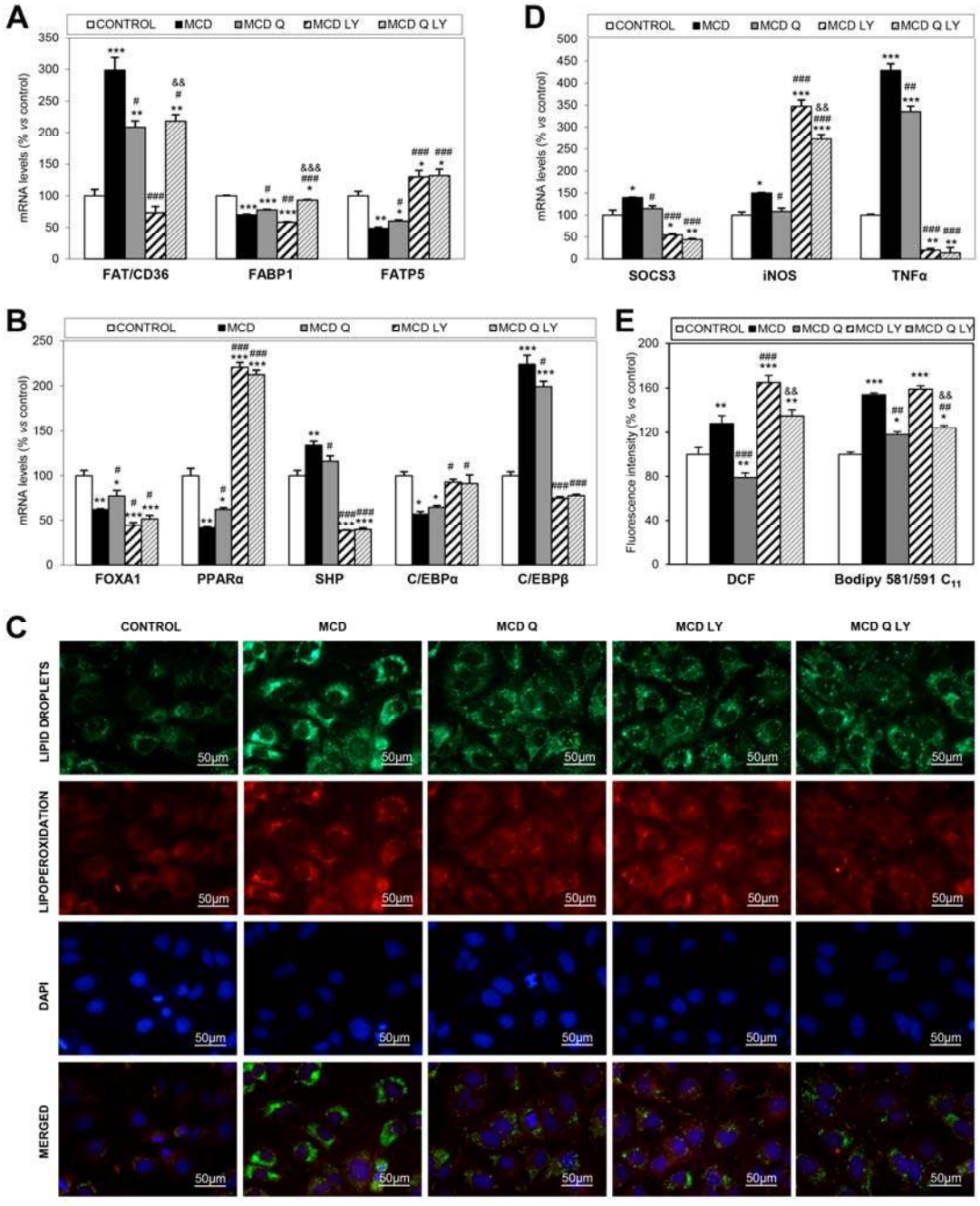
A
CONTROL
MCD
MCD Q
MCD LY
MCD Q LY
mRNA levels (% vs control)
FAT/CD36
FABP1
FATP5
D
SOCS3
iNOS
TNFα
B
FOXA1
PPARα
SHP
C/EBPα
C/EBPβ
E
Fluorescence intensity (% vs control)
DCF
Bodipy 581/591 C11
C
LIPID DROPLETS
LIPOPEROXIDATION
DAPI
MERGED
50µm

Figure 8

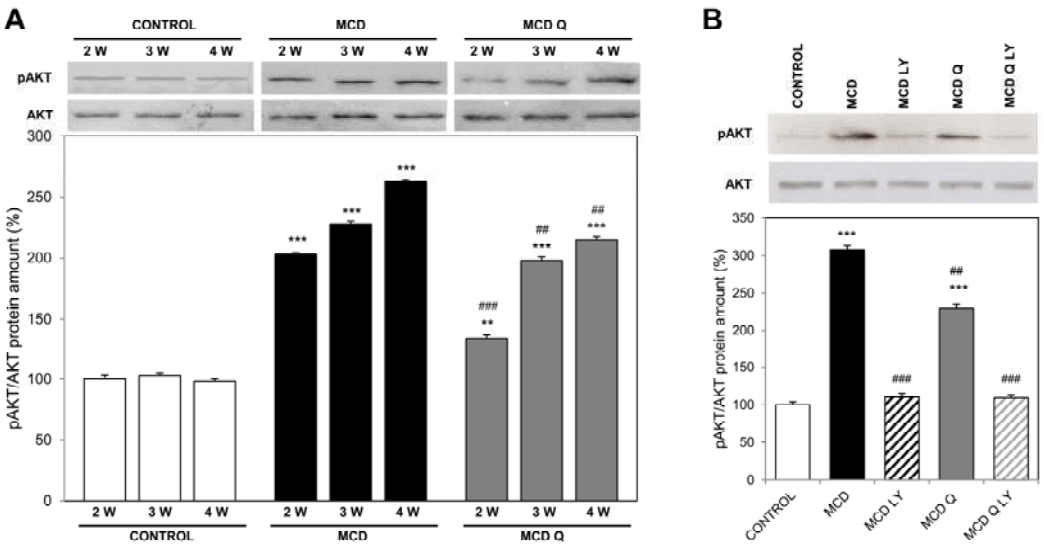
A
CONTROL
MCD
MCD Q
2 W
3 W
4 W
pAKT
AKT
pAKT/AKT protein amount (%)
300
250
200
150
100
50
0
***
**
###
##
B
CONTROL
MCD
MCD LY
MCD Q
MCD Q LY
pAKT
AKT
pAKT/AKT protein amount (%)
350
300
250
200
150
100
50
0
***
##
###

Figure 9

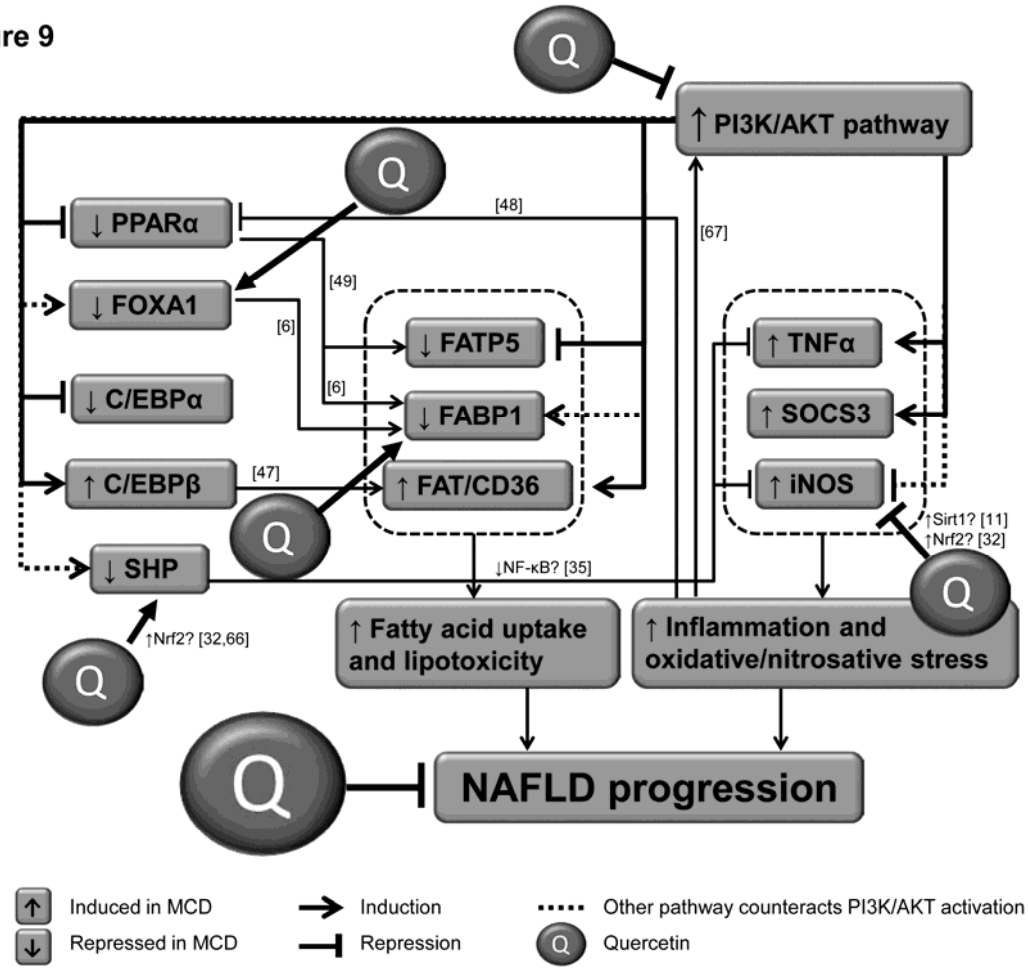
Q
↑ PI3K/AKT pathway
[48]
[67]
↓ PPARα
[49]
↓ FOXA1
[6]
↓ FATP5
↑ TNFα
[6]
↓ C/EBPα
↓ FABP1
↑ SOCS3
↑ C/EBPβ
[47]
↑ FAT/CD36
↑ iNOS
↑Sirt1? [11]
↑Nrf2? [32]
↓ SHP
↓NF-κB? [35]
↑Nrf2? [32,66]
↑ Fatty acid uptake and lipotoxicity
↑ Inflammation and oxidative/nitrosative stress
NAFLD progression
Induced in MCD
Repressed in MCD
Induction
Repression
Other pathway counteracts PI3K/AKT activation
Quercetin

Supporting Information Table 1. Primers and probes used for the RT-qPCR.

Gene	Genbank	Assay ID	Amplicon size	Dye
LXRα	NM_001177730.1	Mm00443454_m1	79	FAM™
SREBP-1c	NM_011480.3	Mm00550338_m1	62	FAM™
FAT/CD36	NM_001159555.1	Mm01135198_m1	112	FAM™
FATP5	NM_009512.2	Mm00447768_m1	96	FAM™
FABP1	NM_017399.4	Mm00444340_m1	72	FAM™
FOXA1	NM_008259.3	Mm00484713_m1	68	FAM™
PPARα	NM_001113418.1	Mm00440939_m1	74	FAM™
C/EBPα	NM_007678.3	Mm00514283_s1	99	FAM™
C/EBPβ	NM_009883.3	Mm00843434_s1	159	FAM™
SHP	NM_011850.2	Mm00442278_m1	73	FAM™
TNFα	NM_001278601.1	Mm00443258_m1	81	FAM™
OPN	NM_001204201.1	Mm01204014_m1	64	FAM™
SOCS3	NM_007707.3	Mm00545913_s1	76	FAM™
iNOS	NM_010927.3	Mm00440485_m1	70	FAM™
GAPDH	NM_008084.2	4352339E	107	VIC™
LXRα	NM_005693.2	Hs00172885_m1	78	FAM™
SREBP-1c	NM_001005291.2	Hs01088691_m1	90	FAM™
FAT/CD36	NM_000072.3	Hs01567186-m1	126	FAM™
FATP5	NM_012254.2	Hs00202073_m1	73	FAM™
FABP1	NM_001443.2	Hs00155026_m1	71	FAM™
FOXA1	NM_004496.3	Hs00270129_m1	74	FAM™
PPARα	NM_001001928.2	Hs00947539_m1	126	FAM™
C/EBPα	NM_004364.3	HS00269972_s1	77	FAM™
C/EBPβ	NM_005194.3	Hs00270923_s1	75	FAM™
SHP	NM_021969.2	Hs00222677_m1	87	FAM™

TNFα	NM_000594.3	Hs00174128_m1	80	FAM™
SOCS3	NM_003955.4	Hs01000485_g1	111	FAM™
iNOS	NM_000625.4	Hs00167248_m1	74	FAM™
GAPDH	NM_002046.3	4326317E	122	VIC™

GAPDH, glyceraldehyde-3-phosphate dehydrogenase.

Supporting Information Table 2. Effect of MCD diet and quercetin on body and liver weights.

	2 W			3 W			4 W		
	CONTROL	MCD	MCD Q	CONTROL	MCD	MCD Q	CONTROL	MCD	MCD Q
BW (g)	24.00 ± 1.00	18.17 ± 0.40***	18.00 ± 0.52***	25.67 ± 1.45	16.33 ± 0.49***	17.00 ± 0.26***	26.00 ± 0.58	15.67 ± 0.33***	15.67 ± 0.42***
LW (g)	1.35 ± 0.05	0.72 ± 0.02***	0.72 ± 0.03***	1.30 ± 0.06	0.62 ± 0.03***	0.63 ± 0.05***	1.17 ± 0.03	0.62 ± 0.03***	0.58 ± 0.03***
L/B W (%)	5.63 ± 0.03	3.95 ± 0.04**	3.98 ± 0.10**	5.07 ± 0.07	3.81 ± 0.29**	3.72 ± 0.27**	4.49 ± 0.07	3.94 ± 0.21	3.71± 0.11

Data are means ± SEM (n=6 mice per group). **P<0.01, ***P<0.001 *vs* CONTROL. BW, body weight; LW, liver weight.

Supporting Information Table 3. Effect of MCD diet and quercetin on plasma biochemical parameters.

	2 W			3 W			4 W		
	CONTROL	MCD	MCD Q	CONTROL	MCD	MCD Q	CONTROL	MCD	MCD Q
AST (U/l)	101±4	402±9***	437±11***	82±5	461±12***	459±16***	107±8	490±9***	483±8***
ALT (U/l)	37.5±2	397±13***	393±9***	30.2±2	479±15***	362±12***#	30.6±2	665±15***	532±16***#
Albumin (g/l)	12±2.2	16.4±0.5	16.2±0.7	14.7±0.6	15.8±0.4	15.5±0.7	14.3±1.2	15.1±1.5	12.6±1.1
Glucose (mg/dl)	299±12	191±7*	192±7*	322±16	147±17***	144±15***	265±4	83±3***	132±7**#
TC (mg/dl)	76±1.5	38.7±1.4***	36.1±2.74***	85.7±2.2	30.4±3.5***	29.5±2.9***	78.4±5.1	23.7±1.3***	31.3±1.3***
HDL (mg/dl)	37±3.4	13.4±0.5***	13.8±1.6***	41±2.4	9±0.6***	10.3±0.7***	37±2.7	7.6±1.1***	9.3±0.5***
LDL (mg/dl)	4.7±0.3	2.4±0.2**	2.1±0.1**	4.5±0.3	1.4±0.1***	1.5±0.1***	4.7±0.3	1.4±0.2***	1.6±0.1***
TG (mg/dl)	80±1.2	41±1.9**	41±1.7**	80±6.6	40.6±3**	52±3.1**#	75±7.8	18.6±4.1***	36.3±2.1**#

Data are means ± SEM (n=6 mice per group). *P<0.05, **P<0.01, ***P<0.001 *vs* CONTROL; #P<0.05 *vs* MCD.